Nuclear Physics News

NuPECC   EUROPEAN SCIENCE FOUNDATION

Volume 19/No. 2

Editor: Gabriele-Elisabeth Körner

Editorial Office: Physikdepartment, E12, Technische Universitat München, 85748 Garching, Germany, Tel: +49 89 2891 2293, +49 172 89 15011, Fax: +49 89 2891 2298, E-mail: sissy.koerner@ph.tum.de

Advanced Diamond Particle Detectors

Introduction

Since the early nineties of the last century, artificial diamond materials grown on various substrates by Chemical Vapour Deposition (CVD) of carbon-containing radicals are being investigated for the detection of ionizing radiation in particle and nuclear physics research. The original motivation was the expected and meanwhile confirmed radiation hardness of CVD diamond (CVDD) [1] required for vertex detectors of the Large Hadron Collider (LHC) experiments at CERN. It was soon recognized that the unique properties of diamond sensors are attractive for many scientific and technological fields.

Diamond is a wide band gap material ($E_g^{Dia} = 5.48\,eV^{T=300\,K}$) combining distinct electronic properties with distinct thermal management. It reveals a high mobility for both charge carriers ($\mu^e = 1800\,cm^2/Vs$, $\mu^h = 2450\,cm^2/Vs$ [2]), a low dielectric constant $\varepsilon_r = 5.7$, and an enormous high breakdown field $\cdot\,10^7$ V/cm. Thermal spikes in diamond are restricted due to a thermal conductivity of $20\,Wcm^{-1}K^{-1}$, which is six times higher than of copper.

CVDD detectors are particularly in demand where classical sensors fail. For instance, in nuclear physics experiments with high-intensity beams, where the detectors have to cope with the serious damage caused by Heavy Ions (HI) measuring simultaneously ion rates up to 100 MHz per detector channel. Depending on energy and nuclear charge Z of the impinging particles, silicon sensors and plastic scintillation counters operate properly up to $\sim 10^7 – 10^9$ HI/cm^2. Radiation hard gas chambers are slow and saturate at high ion rates. In reactor physics, flux monitoring in the vicinity of a reactor core overtax standard neutron detectors (fission chambers, gas counters, and silicon sensors). No traditional detector material withstands the thermal heating loads of synchrotron white beams and the ablation energies involved in XFELs. Due to the wide band gap, diamond detectors are "solar-blind," and therefore ideal for space experiments. Finally, due to the favorable equivalence of carbon with human tissue, CVDD detectors are useful for dosimetry and dose-profile monitoring in tumor therapy with light ions and protons.

CVD-Diamond for Detector Applications

In contrast to gemstones or to crystals synthesized by High-Pressure-High-Temperature (HPHT) processes, diamond plates produced by CVD show excellent electronic properties and highest chemical purity. The crucial issue in this case is the reproduction of the homogeneous crystal structure of natural diamond, which is a common feature of HPHT material.

The worldwide leading industry producing highest quality CVDD is Element Six Ltd., Ascot, Berkshire, UK, and the exclusive distributor of this material is Diamond Detectors Ltd., Poole, Dorset, UK. The denominations of CVDD type and quality used in this report were introduced by these companies. Another commercial producer with remarkable development in recent years is Diamond Materials (DM) in Freiburg, Germany—an SME spin out of the Institut für Angewandte Festkörperforschung (IAF) of the University of Freiburg. Several European, American, and Japanese scientific groups are involved in diamond production and research as well.

Figure 1 shows a simplified schematic of the CVD process applied for diamond growth. CVDD for detector applications ("electronic grade") is synthesized in reactor chambers, where a gas mixture consisting of 98–99% hydrogen and 1–2% methane flows over a substrate fixed at the bottom of the vessel. The flowing gas is activated by microwave excitation. On its drift toward the substrate, complex chemical reactions take place creating, among others, methyl radicals, atomic carbon, and atomic hydrogen. Various carbon phases start to grow on the substrate (illustrated on the left hand side of the figure)— preferably graphite, and a small amount of diamond nuclei. During the whole growth process a stable plasma glows at constant temperature ($\sim 800^{\circ}C$) and pressure (~ 700 mbar) above the substrate, and the aggressive atomic hydrogen destroys instantaneously all carbon phases created except diamond.

The crucial CVDD production steps are the dense and homogeneous diamond nucleation over the substrate
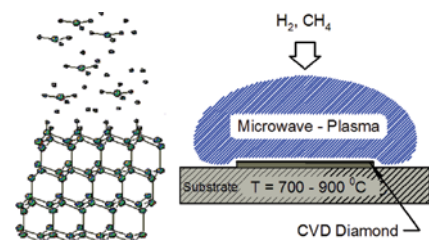

Figure 1. *Schematic of CVD diamond growth process. (Courtesy of Christoph Wild, IAF Freiburg, Germany.)*

facilities and methods

area and the subsequent growth of the first diamond nanolayers, where the lattice constant d_{Sub} of the substrate is consecutively copied and successive adapted to the diamond lattice ($d_{Dia} = 3.567$ Å). A significant mismatching of the lattice constants is the reason for the polycrystalline diamond growth on hetero substrates. The microscopic pictures shown in Figure 2 (from left-to-right: growth side, cross-section, nucleation side) illustrate the surface morphology of an "as grown" (non-polished) sample of 120 μm thickness grown on {100} Silicon ($d_{Si} = 5.431$ Å) after removal of the substrate via etching. The pigmentation of the pictures is an artefact of the photographic emulsion. CVDD is colorless and transparent.

The conically shaped single-crystal diamond grains achieve at growth side dimensions of about 10% of the sample thickness. By lapping several hundreds of micrometers diamond from the nucleation side, more homogeneous material is obtained—historically denominated "detector grade" polycrystalline CVDD. A small amount of nitrogen added to the gas mixture promotes the {100}-growth orientation of the grains (empiric result). Thereby it has to be considered that nitrogen atoms form charge-trapping centers, which reduce the lifetime of the charge carriers. p-conductive CVDD is produced by doping with boron gas in the plasma. The balance between the nitrogen (deep donor) and the boron (acceptor) concentration defines eventually the rest conductivity of CVDD plates.

"Intrinsic" (non-doped) material of highest optical and electronic quality grows on HPHT single-crystal diamond substrates, a few micrometers or less per hour. Imperfections of the substrate surface may build up as isolated structural defects within the CVDD layer, occasionally developing to threading dislocations that reduce the break-down field of the sensors [2].

Figure 3 shows the detector response obtained by scanning single-crystal CVDD (quadrant sensor plotted on the right) with a 6-keV X-ray micro beam at the ESRF in Grenoble [3]. Besides the strong yield from the electrode edge, a homogeneous map of the collected charge is obtained, flat within 3% over the sample area.

Polycrystalline material is available from tenths of micrometers up to 1.5 mm thickness and a maximum size of 4 inches, whereas single-crystal samples are presently released with a maximum area of ~5 mm × 5 mm and thickness from 200 to 500 μm. Special single-crystal diamond is produced up to 1 cm × 1 cm size [1] and down to 40 μm thickness. A promising course for 4-inch wafers of "quasi" single-crystal CVDD is heteroepitaxial growth on iridium [4,5]—a metallic substrate of $d_{Ir} = 3.834$ Å based on the multilayer structure Ir/YSZ/Si(001).

Influence of the Crystal Structure

The high atomic packing factor of the carbon atoms in the diamond lattice has two important consequences: strong covalent bonds being most likely the key to the observed radiation hardness of diamond, and a wide band gap predicting favorable detectors of very low dark current without the need of pn-junction or cooling. The intrinsic carrier density of diamond at 300 K amounts to $N_i \approx 10^{-27}/$ cm^3, which is about thirty orders of magnitude lower than of pure silicon ($E_g^{Si} = 1.12$ eV$^{T=300K}$). At room temperature and operation bias the dark current per mm^2 CVDD amounts to several picoamps for single-crystals and about a factor of 10 higher for polycrystalline material.

In 1932, Karl Hecht [6] investigated the transit of ionized charge through biased crystals in the presence of trapping centers and discovered that the number of collected electrons decreases exponentially with the distance of charge generation to the anode. He introduced the "Schubweg" as the average charge-carrier drift distance $w_x(E)$ in the direction of the
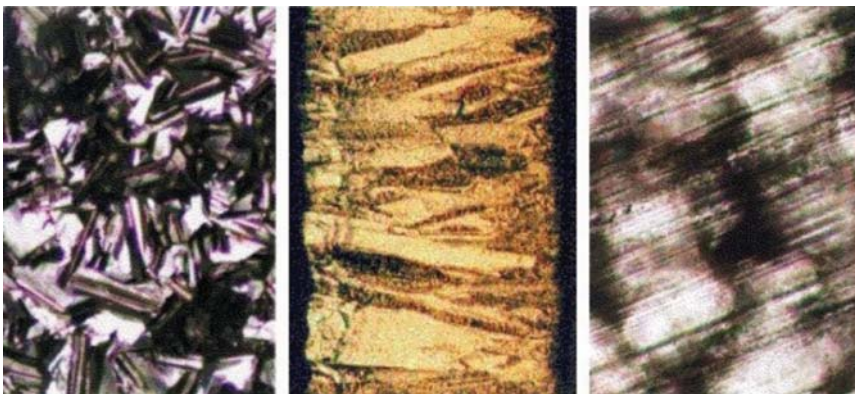

Figure 2. *Surfaces morphology of a typical "as grown" polycrystalline sample (left-to-right): growth –, edge –, and nucleation side.*
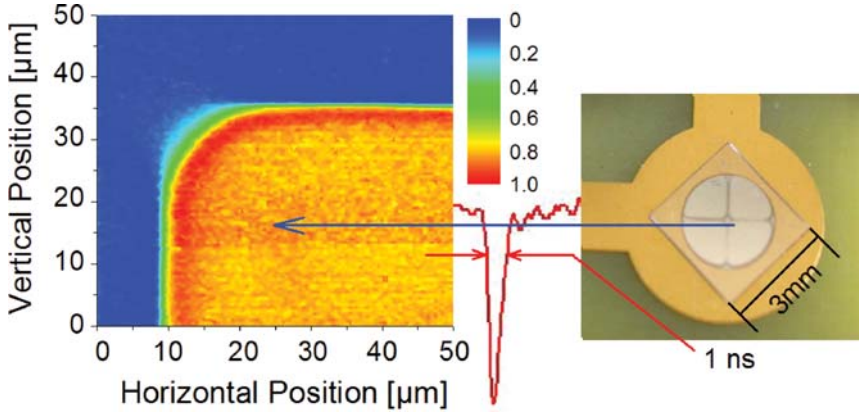
Figure 3. *Mapping (left) of a single-crystal CVDD quadrant sensor (right) with a 6-keV X-ray submicron beam, which confirms the homogeneity of the crystal structure. (Courtesy of John Morse, ESRF.)*

external E-field, at which the number of collected electrons has decreased to 1/e of the generated charge. The value $1/w_x(E)$ can therefore be understood as an E-field dependent absorption constant. Hecht's Eq. (1)

$$\frac{Q_C}{Q_G} = CCE(E)$$
$$= \frac{w_x(E)}{d_D} \cdot \left(1 - e^{\frac{-x}{w_x(E)}}\right) \quad (1)$$

with $w_x(E)$ the Schubweg, d_D the detector thickness, and Q_C, Q_G the collected and the generated charge, respectively, describes the Charge-Collection Efficiency (CCE) of crystal detectors. The message is that a CCE equal to unity is impossible for real sensors. The collected charge Q_C amounts to $0.632 \cdot Q_G$ for $w_x(E) = d_D$ and to $Q_C = 0.995 \cdot Q_G$ for $w_x(E) = 100 \cdot d_D$. Hecht confirmed a proportional increase of $w_x(E)$ with E for small $w_x(E)$ values, and a saturation of the collected charge $Q_C(E)$ at $w_x(E)$ values much larger than the crystal thickness.

He interpreted this observation as the approximate loss-less collection of the generated charge at very high fields. Furthermore, he confirmed for the first time a significant improvement of $w_x(E)$ after blue-light irradiation of the investigated crystals. This effect, known at present as "priming" or "pumping" of low-quality detectors (e.g., polycrystalline CVDD sensors), is explained as a passivation of traps by exposure of the samples to weakly ionizing traversing particles. However, even at "pumped state" and highest bias, polycrystalline detectors show an incomplete charge collection ranging from $0.2 \cdot Q_G$ to $0.6 \cdot Q_G$, whereas single-crystal sensors show a high-efficiency flat "plateau" at rather low electric fields $E_D \sim 0.1$ V/µm.

Charged-Particle Detectors

A CVDD detector consists of a metallized intrinsic diamond plate of thickness d_D biased with a positive or negative DC voltage $V_b = E_D \cdot d_D$, where E_D is the external electric field applied in the {100} growth direction

of the crystal. Diamond sensors operate as fast solid-state ionization chambers, responding to impinging radiation with the generation of N electron-hole pairs (e-h) carrying the charge Q_G, where $N = \Delta E / \varepsilon_{Dia}$ is given by the ionizing energy loss ΔE of the particle and the energy $\varepsilon_{Dia} = 12.84$ eV required to create one e-h in diamond. The original shape of the diamond signal dominated by very high frequencies is maintained using low-noise broadband amplifiers (DBA, Diamond Broadband Amplifiers) [7] and a DSO of a bandwidth ≥ 3 GHz. Figure 4 illustrates the response of a diamond detector assembly after excitation by a charged particle. The detector capacitance C_D loaded with $\pm Q_b = C_D V_b$ discharges promptly due to the separation of the e-h pairs by the electric field (signal rise time). A transient current $I_{tr}(t) = dQ(t)/dt$ flows in the circuit, partially coupling via C_C into the amplifier and partially flowing through the power supply recharging the electrodes with a time constant $R_b C_D$. The biasing current I_b compensates the consumed charge until the circuit is back to equilibrium. For high-rate measurements, the bias resistor R_b is optimized to ensure constant voltage on the electrodes at all times, and V_b to enable a rapid reloading of the electrodes by $C_D \cdot V_b \gg Q_G$.
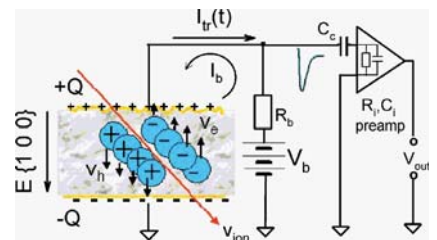

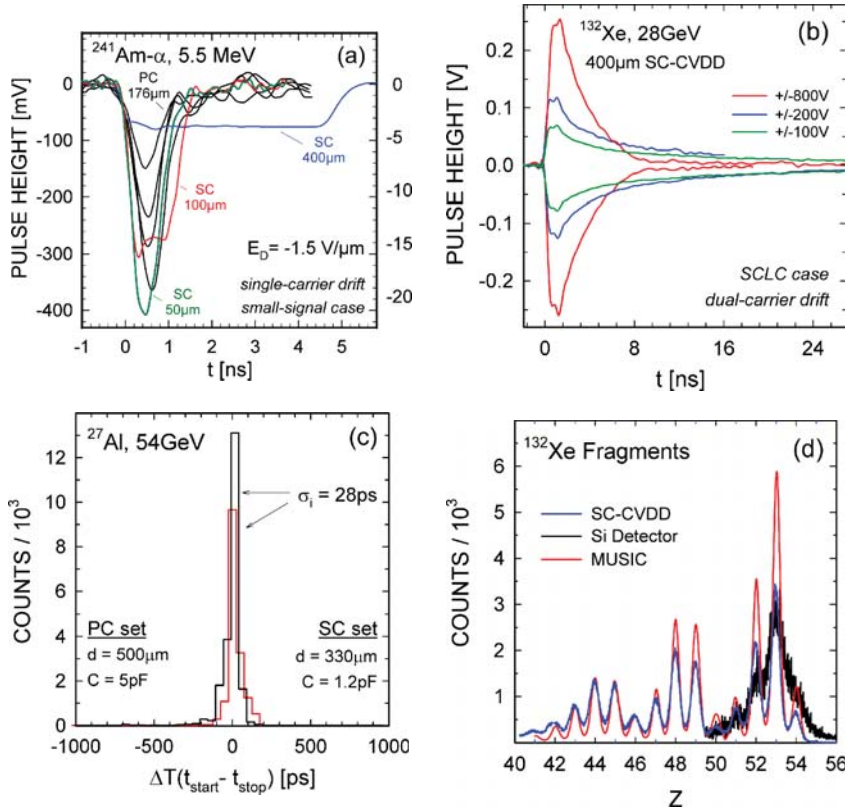**Figure 4.** *The principle of operation of a CVDD (time) detector.*

Figure 5. *(a)* ^{241}*Am-α-transients, measured at constant field with an "as grown" polycrystalline (black traces)—and with three single-crystal diamond sensors (green, red, and blue traces) of different thickness. (b) Relativistic* ^{132}*Xe-transients, measured with a single-crystal CVDD detector of 400 μm thickness at different positive and negative bias. (c) ToF spectra (FOPI) of relativistic* ^{27}*Al ions measured with polycrystalline- (red) and single-crystal (black) diamond sensors, respectively. (d)* ^{132}*Xe fragments measured at the FRS with "spectroscopic grade" CVDD sensors (blue) and a MUSIC detector (red) in the range 41 < Z < 54, and with a silicon detector of 400 μm thickness (black).*

The external electric field deviates from the internal field in case of impurities and structural defects of the diamond crystal. Short-range ^{241}Am-α-particles (range in diamond ~12 μm) are excellent probes for the evaluation of the internal electric field and of the transport parameters of electrons and holes in diamond, because they provide "single-carrier drift" in the "small-signal" case.

Figure 5(a) shows characteristic α-signals of a polycrystalline sensor of 176 μm thickness (triangular black traces) and three single-crystal CVDD sensors of thicknesses 50, 100, and 400 μm, respectively (green, red, and blue traces). The flat-top of the colored trapezoidal pulses predicts a constant internal field as well as a loss-less electron drift to the anode, confirming the homogeneous defect-free crystal

structure of single-crystal CVDD. The field-dependent FWHM of the signals, which corresponds to the transition time t_{tr} of the generated charge-cloud center to the collecting electrode, increases linearly with detector thickness. The drift velocities at 2 V/μm amount to $v_{e,h} = d_D/t_{tr} = 140$ μm/ns for holes and 100 μm/ns for electrons, respectively. The signal area $A = \int U_{tr}(t) \cdot dt$ is proportional to the collected charge $Q_C = (1/R_i) \cdot A$ and for single crystals equal to the generated charge Q_G at all times.

In contrast, the triangular signals of varying amplitude and width measured with the polycrystalline sensor demonstrate an inhomogeneous crystal structure, where random charge loss and recombination occurs. The spread of the drift velocities $v_{e,h}$ and of the deep-trapping lifetimes $\tau_{e,h}$ leads eventually to a Schubweg $w_x(E) = v_{e,h} \cdot \tau_{e,h} = \mu_{e,h} \cdot E \cdot \tau_{e,h}$, which is much shorter than the crystal thickness. However, as far as the signal amplitudes are above discriminator threshold, the restricted charge drift in this sensor type enables HI counting up to ~1 GHz per detector channel.

Figure 5(b) shows original non-amplified Transient Current (TC) pulses induced from ^{132}Xe ions of 28 GeV in a single-crystal detector of 400 μm thickness and 0.9 pF capacitance. The response of the relativistic heavy particles represents the "dual-carrier drift" in the so-called Space-Charge-Limited-Current (SCLC) mode. As expected, the relaxation time in case of SCLC transition (~10 ns) is longer than the decay time of the circuit (45 ps). Nevertheless, the ultra-fast signal rise time remains the same as in the "small-signal" case (≤200 ps) while the FWHM decreases below 3 ns. Figure 5(c) shows ToF spectra obtained with relativistic ^{27}Al ions of 2 AGeV using polycrystalline (red
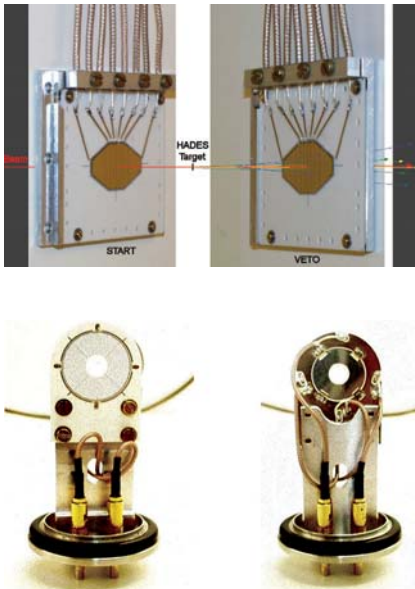
Figure 6. *The start and veto device (top) and the Beam-halo ring counter (bottom, front and back side) of the HADES spectrometer.*

cover consecutive Z ranges. At least for $Z > 50$, we found the Z resolution of "spectroscopic grade" CVDD superior to that of silicon sensors. The reason is that the high pair-production energy of diamond in conjunction with the fast charge collection is in the HI case advantageous, because the generated charge in diamond is less and the relaxation time is shorter than in silicon counters. The integration time of shaping electronics (>500 ns) is still much larger than the diamond relaxation time in the SCLC case (Fig. 5b), in contrast to silicon sensors where signals deteriorate due to such pulse-height defects.

Moreover, diamond sensors (and MUSIC detectors) are insensitive to high-energetic δ-electrons involved in such experiments. The measured line widths δE in the diamond detector case are on the order of the theoretical energy-loss straggling and the energy

resolution $δE/\Delta E = 0.013$ is unexpectedly similar to the resolution of the MUSIC chamber.

Diamond Detectors for GSI and FAIR

Beam intensity and beam profile monitors consisting of polycrystalline CVDD are excellent HI beam diagnostics detectors, operating in single-particle counting mode at beam intensities ranging from single particles to 10^9 ions/s. Such sensors are without competition in the high-frequency time-structure analysis of fast and slow extracted HI beams [7]. However, in the case of highly focused beams single-crystal devices are required.

CVDD sensors monitoring the micro structure of UNILAC beams are implemented in the investigations of hot and dense plasma matter (PP), and

line) and single-crystal CVDD sensors (black line), respectively. The equal intrinsic time resolution of 28 ps obtained from detector sets of such different quality confirms the conclusion that the electronic noise is presently the limiting factor of the excellent time resolution of CVDD detectors.

In a ^{132}Xe fragmentation experiment at the FRS of GSI [8], we compared the energy-loss resolution of CVDD sensors (blue line) with the resolution of a MUSIC chamber (red line) in the ion range $42 < Z < 54$ and with the resolution of a silicon detector (black line) in the range $50 < Z < 54$, respectively (Fig. 5d). Charge-sensitive preamplifiers and shapers are used for these measurements. The periodic variation of the fragment intensities in the spectra is due to the individual transmission profiles of the FRS settings, chosen to
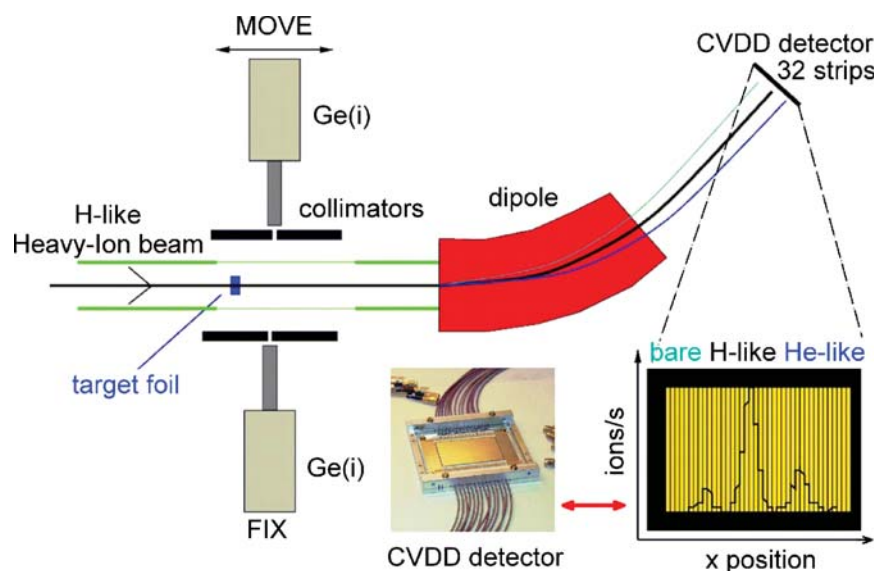

Figure 7. *Setup for atomic physics studies in Cave A (SIS). The CVDD strip detector (6 cm × 4 cm, 32 strips). The photo below the dipole is the focal-plane detector of the HI magnet spectrometer.*

for bunch-length monitoring at HITRAP (AP). Thin single-crystal plates are prepared for long-term spectroscopic monitoring of beam-energy and target quality in medium-energy experiments at SHIP (SHE). Rather important are CVDD start detectors placed in the primary ion beam in order to define the time-zero of a reaction of interest out of, for example, 10^9 collisions/spill. One early successful example is the Start and Veto device of the HADES spectrometer shown on top of Figure 6. It consists of two polycrystalline diamonds of identical octagonal shape and $100\,\mu m$ thickness, placed upstream—respective downstream the HADES target. Each sensor contains eight stripes of variable width, optimized for constant strip rate and a Veto efficiency of 96%. The intrinsic ToF resolution achieved for HIs was below 30 ps. Start detectors for relativistic protons (HADES, FOPI, CBM) are made of single-crystal diamond plates and show at present a time resolution of 107 ps.

Another useful detector is a diamond ring counter installed in the beam line upstream the HADES Start detector as a beam-halo veto counter (Figure 6, bottom; (left) front and (right) back view).

The worldwide largest CVDD detector in operation is the focal-plane detector of the ion spectrometer for atomic physics studies at the SIS (Figure 7). The position-sensitive sensor of $6\,cm \times 4\,cm$ area and $200\,\mu m$ thickness enables ionic charge-state spectroscopy and life-time measurements of hydrogen- and helium-like projectiles up to the heaviest ions. Polycrystalline strip detectors are also foreseen for the upgrade of present charge-exchange detectors (MWPC) at the ion-storage ring ESR including a high-vacuum design for in-ring operation (AP).

Large-area position-sensitive carbon dosimeters for ion-therapy purposes (BIO) operate as fast single-particle beam-monitoring devices. The detection efficiency for ^{12}C ions of therapy energies (80–400 AMeV) was measured to ≥95% for the lowest energy [9]. Significant improvement is expected using single-crystal CVDD detectors of ~100% detection efficiency. However, for absolute dose measurements (counting plus energy measurements including the energy deposition of secondary particles) novel front-end electronics is required capable of high-resolution spectroscopy at ion therapy rates (~50 MHz).

A variety of CVDD sensors are projected for FAIR experiments. The NUSTAR@FAIR group is preparing polycrystalline detectors for tracking and ToF of exotic HI through the SFRS up to the R3B target. The in-beam detectors will operate at rates of 10^7–10^8 ions/s providing all coordinates (x, y, z, t) with sufficient resolution (Δx, Δy, $\Delta z \approx 100\,\mu m$; $\Delta ToF < 50\,ps$). Polycrystalline ToF detectors will also be implemented in the LYCCA spectrometer (HISPEC), whereas for the low-energy branch of the SFRS single-crystal ΔE-E and ToF devices are

considered. In contrast to these HI systems, the position resolution of the CBM vertex detector is required on the order of $3\,\mu m$, and the material budget must be optimized at the lowest acceptable limit. For this application we will explore the potential of large-area quasi single-crystal CVDD grown on iridium, in particular novel strip-detector designs read out with PADI ASICs [10].

X-Ray Beam Monitors

Bunched X-ray beams at third generation synchrotron facilities are now routinely focused to diameters <1μm.

Detectors of similar precision are required either to monitor beam position and bunch time structure or to provide real-time information for position control. Diamond has a very low absorption coefficient over the X-ray energy range 5–20 keV, and it is therefore an outstanding material for the fabrication of "semitransparent" monitors that may be left *in situ* for continuous feedback [3]. Encouraging test measurements have been performed at the ID21 beam line of the ESRF using the sector sensor of $50\,\mu m$ thickness shown in Figure 3. The plotted current
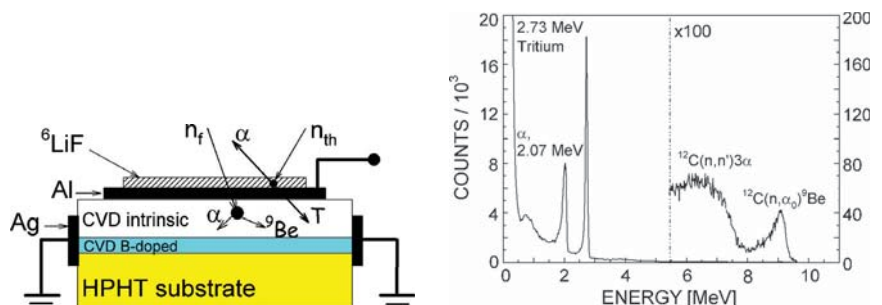

Figure 8. *(left) CVDD neutron detector simultaneously detecting thermal and fast neutrons. (right) Thermal-neutron (left graph) and fast-neutron spectra (right graph), respectively. (Courtesy of Gianluca Verona-Rinati, University Roma Tor Vergata.).*

signal of <1 ns width is obtained from one X-ray bunch of ~50 ps duration, readout with a DBA. The sensitivity of the device to beam movements was <20 nm.

Neutron Detectors

Single-crystal CVDD detectors with ^{6}LiF coating are capable of simultaneous measurement of thermal neutrons via the reaction ^{6}Li(n,α)T and fast neutrons via the reaction ^{12}C$(n,\alpha)^9$Be (Figure 8) [11]. Such n-flux monitors can operate in a distance of 1 m to the reactor core. Since February 2006, two neutron detectors of this kind are installed at JET (Joint European Torus) and connected to the main on-line data acquisition system. They are continuously working in normal operating conditions, showing extremely stable performance. Similar devices are foreseen for ITER.

Of general interest striving for reliable diamond detector electrodes is the feature of the thin highly boron-doped CVDD layer indicated in cyan, which is grown before deposition of the sensing film.

Concluding Remarks

The versatile CVDD sensors are ideal front-end detectors meeting most of the requirements of new-generation nuclear physics experiments and other advanced applications. They are robust, ultra-fast, low background sensors, available in various thickness and shape. The high pair-production energy in diamond complicates MIP measurements but is advantageous for the detection of highly ionizing ions. Stopped particles polarize the inhomogeneous detector material of polycrystalline sensors and should be therefore detected with single-crystal devices. For timing of swift ions, thin "as grown" polycrystalline sensors are superior to "spectroscopic grade" counters, in contrast to any application based on ΔE-E spectroscopy for which this type of CVDD cannot be used. The small size of single-crystal plates is a drawback considering large-area MIP-tracking detectors. However, it has been demonstrated that its actual size and quality suit excellently for many other important sensor categories. The next step forward in the development of advanced diamond detectors is expected from the novel large-area CVDD material grown on iridium, and from improved front-end electronics for diamond detectors.

References

1. RD42 Collaboration, Status Report, CERN/LHCC 2008-005.
2. M. Pomorski, *PhD Thesis*, University of Frankfurt (2008).
3. J. Morse et al., *Proc. MRS Fall Meeting* (2007), Boston, MA, USA.
4. S. Gsell et al., *Appl. Phys. Lett.* 84 (2004) 4541.
5. A. Stolz et al., *Diam. Rel. Mater.* 15 (2006) 807.
6. K. Hecht, *Zeitschrift für Physik* 77 (1932) 235.
7. P. Moritz et al., *Diam. Rel. Mater.* 10 (2001) 1765.
8. E. Berdermann et al., *XLV Int. Winter Meeting* (2007) Bormio.
9. M. Rbisz, *PhD Thesis*, University of Heidelberg (2008).
10. M. Ciobanu et al., *Proc. IEEE NSS Cont. Rec.* N30–18 (2008) 2018.
11. S. Almaviva et al., *J. Appl. Phys.* 103 (2008) 054501

ELENI BERDERMANN FOR THE NORHDIA COLLABORATION
GSI Helmholtz Zentrum für Schwerionenforschung GmbH